HHS Public Access

Author manuscript

Biomed Pharmacother. Author manuscript; available in PMC 2022 November 01.

Published in final edited form as:

Biomed Pharmacother. 2022 November ; 155: 113843. doi:10.1016/j.biopha.2022.113843.

Histone deacetylase inhibitors enhance oncolytic herpes simplex virus therapy for malignant meningioma

Yoichiro Kawamura[a,1], **Lingyang Hua**[a,b,1], **Alessandra Gurtner**[a,1], **Ego Wong**[a], **Juri Kiyokawa**[a], **Nadia Shah**[a], **Joshua Gorham**[c], **Hiroko Wakimoto**[c], **Samuel D. Rabkin**[a], **Robert L. Martuza**[a], **Hiroaki Wakimoto**[a,*]

[a]Department of Neurosurgery, Massachusetts General Hospital, Harvard Medical School, Boston, MA 02114, USA

[b]Department of Neurosurgery, Huashan Hospital, Fudan University, Shanghai, China

[c]Department of Genetics, Harvard Medical School, Boston, MA 02115, USA

Abstract

Approximately 20% of meningiomas are not benign (higher grade) and tend to relapse after surgery and radiation therapy. Malignant (anaplastic) meningioma (MM) is a minor subset of high-grade meningioma that is lethal with no effective treatment options currently. Oncolytic herpes simplex virus (oHSV) is a powerful anti-cancer modality that induces both direct cell death and anti-tumor immunity, and has shown activity in preclinical models of MM. However, clinically meaningful efficacy will likely entail rational mechanistic combination approaches. We here show that epigenome modulator histone deacetylase inhibitors (HDACi) increase anti-cancer effects of oHSV in human MM models, IOMM-Lee (NF2 wild-type) and CH157 (NF2 mutant). Minimally toxic, sub-micromolar concentrations of pan-HDACi, Trichostatin A and Panobinostat, substantively increased the infectability and spread of oHSV G47Δ within MM cells *in vitro*, resulting in enhanced oHSV-mediated killing of target cells when infected at low multiplicity of infection (MOI). Transcriptomics analysis identified selective alteration of mRNA processing and splicing modules that might underlie the potent anti-MM effects of combining HDACi and oHSV. *In vivo*, HDACi treatment increased intratumoral oHSV replication and boosted the capacity of oHSV to control the growth of human MM xenografts. Thus, our work supports further

*Correspondence to: Massachusetts General Hospital, 185 Cambridge Street, Boston, MA 02114, USA. hwakimoto@mgh.harvard.edu (H. Wakimoto).

[1]These authors contributed equally to this work.

CRediT authorship contribution statement

Conceptualization: Hiroaki W; Methodology: YK, LH, AG, EW; Experimentation: YK, LH, AG, EW, JK, JG; Data analysis: YK, LH, AG, EW, Hiroko W; Writing – original draft: Hiroaki W, YK; Writing – review & editing: Hiroaki W, YK, EW, NS, SDR, RLM; Supervision: Hiroaki W, SDR, RLM; Funding acquisition: Hiroaki W, RLM. All the authors have read and approved the manuscript.

Conflict of interest statement

SDR and RLM are co-inventors on patents relating to oncolytic herpes simplex viruses, owned and managed by Georgetown University and Massachusetts General Hospital, which have received royalties from Amgen and ActiVec Inc. SDR acted as a consultant and received honoraria from Replimune, Cellinta, and Greenfire Bio, and honoraria and equity from EG 427. RLM. is on the S.A.B. and receives payment from Virogin Biotech Ltd.

Appendix A. Supporting information

Supplementary data associated with this article can be found in the online version at doi:10.1016/j.biopha.2022.113843.

translational development of the combination approach employing HDACi and oHSV for the treatment of MM.

Keywords

Meningioma; Malignant meningioma; Oncolytic herpes simplex virus; Histone deacetylase inhibitor

1. Introduction

According to the Central Brain Tumor Registry of the United States (CBTRUS, 2013–2017), meningioma is the most prevalent tumor type in the CNS, constituting 38.3% of all CNS tumors [1]. Meningioma is a group of heterogenous tumors with differing malignancy and clinical course. The majority (about 80%) of meningioma are WHO grade 1 and considered benign, whereas WHO grade 2 (histologically mostly atypical) and WHO grade 3 (malignant meningioma, MM, histologically mostly anaplastic) comprise 15% and 2–3% of the total, respectively, and are higher-grade meningiomas (HGM). Meningiomas are comprised of genomically diverse groups of tumors [2,3]. About 50% of meningiomas and an even higher fraction of HGM have mutations or inactivation of the tumor suppressor gene *NF2*, for which direct molecular targeting is not currently feasible.

HGMs pose a significant clinical challenge as 40% of grade 2 and up to 80% of grade 3 tumors relapse after surgery and radiation within 5 years. At recurrence HGMs are frequently refractory to repeated surgery and radiotherapy. Although rare, MM is devastating as the tumor relentlessly relapses resisting existing therapies and can be lethal. Unlike many of WHO grade 1 meningiomas, gross total resection does not offer cures in patients with MM. Post-operative radiation therapy has some effect on extending survival of the patients, however MM evades the effects of radiation. Clinical investigations testing systemic chemotherapeutics [4,5] or molecularly targeted agents [6–13] have not improved clinical outcomes. As a result, 5-year-media survival of MM has been reported to be 40–41.4% in recent publications analyzing large cohorts collected from multiple institutions [14,15]. This unmet medical need, however, tends to be overlooked because the better clinical outcomes for the majority of benign meningiomas overshadow the poor outcomes for this relative minority group of MM. Thus, there is a clear and urgent need to develop new and effective treatments for MM.

Oncolytic viruses have unique dual mechanisms-of-action (MOA): 1) direct and selective killing of neoplastic cells and 2) elicitation of inflammatory and anti-tumor immune responses [16]. Oncolytic virus therapy has emerged as a promising modality for cancers, including the lethal malignancies in the brain. Using clinically representative orthotopic models of patient-derived MM and glioblastoma (GBM), we have demonstrated significant anti-tumor effects of oncolytic herpes simplex viruses (oHSV) [17–22]. Clinical development of oHSV is more advanced for GBM treatment as the oHSV G47Δ was recently conditionally approved in Japan [23,24], and no clinical trial for meningioma is active currently. Additionally, monotherapy has been relatively ineffective and it is widely considered that rationally designed mechanistic combinatory approaches involving

oncolytic viruses will be not only more efficacious but necessary to effectively treat refractory malignancies such as GBM and MM. To this end, we have reported combinatorial approaches using transgene arming [18] or targeted agents [17, 25] to augment the activity of oHSV against tumors.

One of the attractive candidates as a therapeutic partner with oncolytic virus are histone deacetylase inhibitors (HDACis). HDAC is a group of epigenome modifying enzymes that are highly expressed in neoplastic cells and play a vital role in a variety of processes including gene expression regulation, cell survival, proliferation, and immune responses [26]. HDACis have been developed as anti-cancer agents, including hydroxamic acids vorinostat and panobinostat that have been approved by the U.S. FDA for the treatment of cutaneous and peripheral T-cell lymphomas and multiple myeloma, respectively [27,28]. Because of its versatile functions to modulate gene expression and innate immunity, HDACis have been studied for their potential to enhance the efficacy of various oncolytic viruses [29,30]. Varying degrees of beneficial effects and mechanistic insights that underlie interactions between HDACis and oncolytic viruses have been reported. However, whether HDAC inhibition can be safely combined with oHSV to enhance therapeutic activity against MM is unknown.

The goal of the current study is thus to address our hypothesis that combining HDACis with oHSV is a rational mechanistic therapeutic strategy against MM. Our investigations employing human MM cells and xenograft models provide experimental evidence that low-dose HDACis can boost the anti-MM activity of oHSV and that the combination warrants clinical evaluation.

2. Materials and methods

2.1. Virus

G47Δ is a multi-mutated oHSV derived from strain F, containing deletions of γ34.5 and ICP47, and LacZ inactivation of ICP6 [31]. G47Δ-Us11fluc is a derivative of G47Δ that expresses firefly luciferase (fluc) driven by the true late Us11 virus promoter [22]. G47Δ-mCherry is a derivative of G47Δ that expresses mCherry driven by the IE4/5 immediate early promoter [32]. oHSVs were amplified in Vero cells and concentrated as described previously [21].

2.2. Cells

African green monkey Vero cells (RRID:CVCL_0059) were from ATCC and grown in DMEM supplemented with 10% calf serum. Human MM cells IOMM-Lee (RRID:CVCL_5779, NF2 intact) and CH157 (CH-157MN, RRID:CVCL_5723, NF2 loss) were obtained from Dr. Randy Jensen (University of Utah) and Dr. Wenya Bi (Brigham and Women's Hospital), respectively, and were cultured in DMEM supplemented with 10% fetal calf serum. These cell lines were authenticated by short tandem repeat analysis (IDEXX) in 2022 (Supplementary Table S1). The result of IOMM-Lee perfectly matched with IOMM-Lee (ATCC #CRL-3370). Reference profile is not available for CH157, but CLASTR search at Cellosaurus identified no match with other cell lines. Normal human

astrocytes were purchased from ScienCell, and used within passage 8. All experiments were performed with mycoplasma free cells.

2.3. Histone deacetylase inhibitors

Trichostatin A and Panobinostat were purchased from Med Chem Express and ApexBio, respectively, and dissolved in DMSO, aliquoted and stored at −20 °C.

2.4. Cell viability assay

In vitro cell viability assay was performed using MTS assay as previously described [33]. Cells were seeded at 1500–3000 cells per well of 96-well plates, followed by exposure to G47Δ or HDACi at doses indicated in the figures. When combination therapy was tested, cells were treated with HDACis first, followed 5 h later with G47Δ. Three or four days later, cell viability was assayed by incubation of cells with MTS for 1–2 h and measurement of absorbance at 490 nm.

2.5. Virus infectability assay

Cells were plated at 12,000 cells per well in 48-well plates, given HDACi at the indicated concentrations in triplicate, followed 5 h later by infection with G47Δ at MOI= 0.3. Six hours later, cells were fixed with 0.5% glutaraldehyde for 10 min. After washed with PBS, infected cells were visualized by staining with 5-bromo-4-chloro-3-indolyl-D-galactoside (x-gal). Microscopic images were captured, and infectability represented by x-gal$^+$ cells was measured using ImageJ (NIH) and presented as % Area.

2.6. Virus yield assay

Cells seeded at 50,000–75,000 cells per well of 24-well plates were treated with and without HDACi and infected with G47Δ. At indicated times, cells and media were collected and subjected to three cycles of freeze and thaw to release virus into supernatant. Virus yield was titrated by plaque assay on Vero cells.

2.7. RNA sequencing

Two million cells were seeded in a 10 cm dish and treated with mock, HDACi, G47Δ or HDACi followed by G47Δ. Treatment doses used were: Trichostatin A (50 nM), Panobinostat (0.3 nM), G47Δ (MOI=0.1) for IOMM-Lee, and Trichostatin A (100 nM), Panobinostat (2.5 nM), G47Δ (MOI=0.5) for CH157. Twenty-four hours after virus infection (29 h after HDACi), cells were collected for total RNA extract using Trizol (Invitrogen). See Supplementary Methods for details.

2.8. Malignant meningioma xenograft studies

Two million IOMM-Lee cells were subcutaneously implanted in the right flank of 7-week-old female athymic nu/nu mice (Charles River Lab). When tumor volume reached about 150 mm3, mice received intraperitoneal injections of Panobinostat at 30 mg/kg or PBS for 2 days in a row. G47Δ-Us11fluc (3×10^5 pfu / 10 μl) was intratumorally injected 5 h after the first Panobinostat injection. D-luciferin was injected intraperitoneally (180 mg/kg), and bioluminescence imaging was performed using SPECTRAL Ami X (Spectral instruments

imaging, Tucson, AZ) under isoflurane anesthesia of mice to measure the activity of fluc as a surrogate of virus replication. To determine the therapeutic activity of combination therapy, tumor size was monitored during and post therapies by caliper measurement, and the tumor volume was calculated based on the longest (L) and the perpendicular (S) diameters of the tumor, using the formula: Volume (mm^3)= 1/2xLxS^2. All studies and procedures involving animals have been approved by the Institutional Animal Care and Use Committee of Massachusetts General Hospital, and in compliance with the institutional guidelines.

2.9. Statistical analysis

Comparisons of data in viral replication and cytotoxicity assays were performed using a two-tailed Student t-test (unpaired) or two-way analysis of variance (ANOVA) with Bonferroni multiple comparisons. All statistical analyses were performed using Prism 9 Software (Graph-Pad, v9.3.1). P values of less than 0.05 were considered significant.

3. Results

3.1. Low dose HDAC inhibitors enhances G47Δ-mediated killing of malignant meningioma (MM) cells in vitro

We first tested human MM cell lines IOMM-Lee and CH157 cells for their sensitivity to oHSV G47Δ *in vitro*. Cell viability assay showed a dose-dependent response of these cells to G47Δ, with IOMM-Lee cells exhibiting obviously higher sensitivity, with 50% inhibitory concentration (IC50) of the 3-day assay being 0.01 and 0.3 for IOMM-Lee and CH157 cells, respectively (Fig. 1AB). These MM cells also responded to two pan-HDACis, Trichostatin A (TSA) and Panobinostat (Pano), in a dose-dependent manner (Fig. 1C, D). Although both HDACis were potently cytotoxic to the MM cells at sub-micromolar concentrations, Pano was more effective than TSA at lower dose ranges. IOMM-Lee cells were more sensitive to these HDACis than CH157 cells, as IC50 for Pano was 7.9 and 20.0 nM and that for TSA was 98.1 and 235.5 nM in IOMM-Lee and CH157 cells, respectively (Fig. 1C, D).

We next tested whether low-dose HDACis could sensitize MM cells to the oncolytic effects of oHSV G47Δ. We chose HDACi doses that are only marginally (5–10%) cytotoxic on their own, yet potentiated the anti-MM activity of G47Δ (Fig. 1E–H). Indeed, this sensitization effect of HDACi was consistently observed with both TSA and Pano in both human MM cell lines that are genetically distinct and displayed differing sensitivity to oHSV-mediated cytotoxicity. Such increased killing by the combination therapy was not observed in normal human astrocytes (Supplementary Fig. S1). Thus, low dose-pan-HDACis enhanced the oncolytic activity of oHSV G47Δ against human MM cells.

3.2. Low dose HDAC inhibitors increase infectability, replication and spread of oHSV G47Δ in MM cells

Next, we determined the HDACi-induced changes in virus-host cell interactions that could underlie HDACi-mediated enhancement of oHSV activity. Pretreatment of MM cells with HDACi significantly increased the entry (*i.e.*, infectability) of G47Δ into MM cells, as measured with x-gal staining of cells 6 h post-infection (Fig. 2A–D), and doses as low as 25 nM (TSA) and 0.75 nM (Pano) were again impactful. Virus yield assay further showed

that exposure to low dose HDACis significantly augmented the replication of oHSV in the two MM cell lines, however the effect was more prominently observed in CH157 cells (Fig. 2E, F). In accord with these results, the spread of G47Δ was also positively impacted by pretreatment of MM cells with HDACis. Exposure to HDACis enabled infection of G47Δ-mCherry to spread more robustly in monolayer cultured MM cells *in vitro*, as compared with infection without HDACis (Fig. 2G, H). Of note, these effects were similarly and consistently mediated by TSA and Pano, supporting the idea that the observed effects were driven by HADC inhibition. Thus, low dose pan-HDACis increase infectability, replication and spread of oHSV G47Δ in MM cells, leading to increased killing of the MM cells.

3.3. Transcriptional changes mediated by the combination treatment of MM cells by HDAC inhibitors and oHSV G47Δ

To understand the molecular underpinnings of the HDACis-mediated enhancement oHSV therapy, we conducted transcriptomics analysis using RNA sequencing. IOMM-Lee and CH157 MM cells were treated with HDACis (either TSA or Pano), followed 5 h later by infection with G47Δ, and harvest of the cells 24 h post-infection for RNA extraction, the timing that ensures completion of at least one oHSV replication cycle and viability of majority of the cells. The coverage and quality of the sequencing data is summarized in Supplementary Table S2. Principal component analysis revealed that mock-treated IOMM-Lee or CH157 MM (IO, CH) control cells (C, 1 and 2 in the plot) and HDACi-treated cells without G47Δ (Hi, 5–8) gathered close together, probably reflecting the limited effect of low-dose treatment (Fig. 3A). However, C or Hi, G47Δ-infected cells without HDACi (G, 3 and 4) and cells co-treated with HDACis and G47Δ (Hi_G, 9–12) displayed good separation (Fig. 3A). Transcriptomics induced by TSA and Pano (Hi) were grouped closely, whether with or without G47Δ, indicating that the two HDACis mediated similar transcriptomic changes (Fig. 3A). Heat map generated with cluster analysis also indicated similar expression patterns induced by the two HDACis (Supplementary Fig. S2). We then shifted our attention to differential gene expression between the Hi_G and G groups to identify the transcriptomic impacts of HDACis in the context of G47Δ treatment of MM cells. We focused our analysis on mRNA changes that occurred commonly in both IOMM-Lee and CH157 cells because such an approach could isolate biological phenomena that are generalizable in HDACi-induced enhancement of oHSV therapy of MM. HDACis conferred more numerous and diverse statistically significant changes in gene expression in G47Δ-treated CH157 cells, as compared with IOMM-Lee cells (Fig. 3B–E), which may reflect robust HDACi sensitization of comparably oHSV-insensitive CH157 cells. Nevertheless, analysis of differentially expressed genes found the gene ontologies pertaining to RNA processing and RNA splicing highly significantly and commonly enriched in the comparisons between the Hi_G and G groups in IOMM-Lee and CH157 cells (Fig. 3D, E) (Supplementary Fig. S3 and Supplementary Table S3). Our results thus suggest that HDACi-induced modification of RNA processing mechanistically underlie HDACi augmentation of oHSV treatment of MM.

3.4. HDACis did not induce consistent changes in interferon-mediated anti-viral responses in MM cells

HDACis including TSA have been shown to inhibit innate anti-viral responses involving interferons and other mechanisms (reviewed in [29,30]). We used our transcriptomics data to examine whether HDACis influence expression of a set of genes previously implicated in HDACis modulation of innate anti-virus responses (Fig. 4) [34–36]. G47Δ infection triggered expression of IRF7, but not IRF3, in both MM cells (Fig. 4A, B). Interestingly, downstream signaling was largely inhibited in oHSV-permissive IOMM-Lee cells as shown by downregulation of multiple interferon-stimulated genes [37], namely IFIT1 and IFIT3, and OAS1, whereas these were either upregulated or unchanged in CH157 cells that are less permissive to oHSV (Fig. 4C–H). In G47Δ-infected IOMM-Lee cells, pretreatment with HDACis did not result in apparent additional inhibition of innate defense genes (Fig. 4C–H), presumably because G47Δ alone effectively blocked the cellular innate response in this MM cell line. In G47Δ-infected CH157 cells, however, we noted some evidence that pre-exposure to HDACis inhibited interferon-related anti-oHSV responses; downregulation of STAT1, IFIT1 and IFIT3 by HDACis (Fig. 4C–E). Furthermore, TSA decreased EIF2AK2 (PKR) and Pano potently decreased PML in G47Δ-infected CH157 cells (Fig. 4F, H). These results suggested that, at least in human MM cells, HDACis-mediated inhibition of oHSV-triggered, interferon-driven anti-viral responses were cell-context dependent.

We and others have shown that changes in expression of cell cycle genes underlie the increased anti-cancer effects of combining HDACis and oncolytic viruses [38,39]. Consistent with these reports, we observed that pretreatment of MM cells with HDACis enhanced G47Δ-induced upregulation of CDKN1A (p21) and downregulation of CCND1 (cyclin D1) (Supplementary Fig. S4).

3.5. HDACi boosted the replication and therapeutic activity of oHSV G47Δ in human malignant meningioma xenografts in vivo

Lastly, we determined the therapeutic impact of HDACis on intra-tumoral oHSV therapy of MM in a mouse xenograft model. To this end, we focused on Pano since TSA is not applicable to clinical use. We first tested if Pano monotherapy would alter the growth of human MM. Two daily systemic administrations of Pano (at 30 mg/kg) in athymic mice were well tolerated and did not impact the growth of IOMM-Lee xenografts as compared with vehicle treatment (Fig. 5A). We then designed an experiment using G47Δ-Us11fluc to assess HDACi-induced enhancement of intra-tumoral replication and therapeutic effects of G47Δ, simultaneously (Fig. 5B). Bioluminescence imaging demonstrated a significant increase (over double on average) of fluc signals emitted from oHSV-injected MM xenografts when combined with Pano (Fig. 5C, D). Although tumor growth was inhibited by intra-tumoral injection of G47Δ-Us11fluc, significantly more potent growth inhibition was observed when Pano was combined with oHSV (Fig. 5E, F). The levels of the fluc signals (on day 3 post G47Δ-Us11fluc injection) negatively correlated with the subsequent changes in tumor volume (on day 10) (Fig. 5G), suggesting a positive correlation between intra-tumoral virus replication and tumor response to oHSV therapy.

4. Discussion

oHSV offers an alternative approach to address the unmet medical need of a lack of effective treatments for HGM. However, mechanistic combinatorial strategies are most likely necessary to counter the notoriously treatment-refractory nature of this cancer type. In this work, we present preclinical evidence that pan-HDACis can enhance the replication and anti-tumor activity of the clinical oHSV G47Δ in human MM models, representing both NF2-mutant and intact tumors, *in vitro* and *in vivo*.

Both TSA and Pano exhibited high cytotoxicity to human MM cells *in vitro* at sub-micromolar dose ranges, direct anti-tumor activity consistent with what was shown in breast cancer cell lines [40]. Pano was previously identified as a potent hit in a screening of an epigenetic compound library tested only at 1 μM final dose in a panel of human meningioma cell models, including IOMM-Lee and CH157 cells [41]. We chose HDACi concentrations that were minimally cytotoxic on their own, in order to isolate their potential to sensitize MM cells to oHSV treatment. We consistently found that low dose HDACis enhanced G47Δ-mediated killing of MM cells, which was associated with increased virus entry, replication and spread. This observation was in line with other reports that have shown beneficial effects of various HDACis on increasing infectivity and/or replication of oncolytic viruses of differing platforms including oHSV [36,40,42], oncolytic adenovirus [43], and vesicular stomatitis virus [35]. Interestingly, our prior published work investigating TSA in modulating G47Δ therapy of cell lines from several cancer types other than MM did not find TSA-induced changes in the degree of G47Δ replication *in vitro* when a rather high dose of TSA (100 ng/ml corresponding to 330 nM) was used [39]. In the current work, we also noted a narrow HDACi dose window elevated virus yield in oHSV-permissive IOMM-Lee cells, as 25 nM TSA, not higher 50 nM, was effective. On the other hand, more consistent and less dose-dependent HDACis effects were observed on virus infectivity and spread. The virus infectivity assay using early virus LacZ expression and x-gal staining as the readout can reflect the efficiency of G47Δ to enter the host cell, traffic to the nucleus, and express LacZ. HDACi-mediated augmentation of virus yield *in vitro* thus appeared to be dependent on multiple factors that include permissiveness of the cancer cells to the virus and the HDACi dose. Our findings with NF2-intact IOMM-Lee and NF2-mutant CH157 models also suggested that the combination benefit does not rely on the tumor's NF2 status, however, this requires experimental validation before drawing a conclusion.

Mechanistically, multiple studies have shown that HDACis enhance the activity of oncolytic viruses including oHSV by suppressing interferon-driven innate anti-viral responses [35,36]. Additionally, we and other have reported that HDACis modulated expression of cell cycle-regulating genes to halt cell cycle progression [38,39]. The HDACis that have been most extensively studied so far are TSA (pan HDACi) and valproic acid (Class I and IIa HDACi), and both seem to drive similar mechanisms to enhance oncolytic viruses. In this work, principal component analysis of RNA sequencing data revealed that combining low dose TSA or Pano with G47Δ mediated similar transcriptomics changes in the transcriptomic landscape of G47Δ treatment alone, supportive of the drug effects being due to on-target inhibition of HDACis. CH157 cells responded to HDACis and G47Δ with changes in a much larger number of transcripts than IOMM-Lee cells. A search for differentially

expressed gene ontology modules identified mRNA processing and mRNA splicing GO to be significant in both IOMM-Lee and CH157 cells. When combined with G47Δ, HDACis consistently altered a set of genes coding for proteins participating in mRNA processing that involves addition of the 5′ cap and a 3′ poly (A) tail and pre-mRNA splicing. This is an unexpected discovery since HSV, relying on host transcription and RNA processing machinery to express viral RNAs, has evolved measures (*via* immediate early genes, ICP4, ICP22 and ICP27, all present in G47Δ) to antagonize multiple cellular transcriptional events in favor of its own gene expression [44]. ICP27 has been shown to interact with splicing factors such as SRSF1, SRSF2, and SRSF7 [45–47] that were found to be downregulated (SRSF1) or upregulated (SRSF2 and SRSF7) when MM cells were exposed to HDACi before oHSV infection (Supplementary Table S1). Our finding that HDACis enhancement of oHSV was consistently associated with mRNA processing supports the unique capacity of HDACis to optimize HSV-driven aberrant mRNA processing of cellular genes, and ensure virus mRNA processing and export, resulting in the augmentation of oHSV replication. Our results, however, do not exclude the role of other mechanisms; in fact, our transcriptomics analysis showed HDACi-mediated suppression of innate anti-viral responses in CH157 cells.

TSA and Pano displayed comparable properties to enhance oHSV therapy of MM *in vitro*. We selected Pano for *in vivo* studies with MM xenografts, since Pano was approved for the treatment of multiple myeloma, while TSA is a preclinical agent [27]. Using a G47Δ variant expressing fluc driven by an HSV true late promoter, we show that systemic treatment with Pano increased intratumoral replication of G47Δ injected into IOMM-Lee MM, which was associated with superior tumor growth inhibition. We also show that non-invasive bioluminescence imaging and quantitation of virus replication had a utility to predict subsequent, better tumor control. Previously, HDACis of different classes, namely valproic acid (class I and IIa), entinostat (class I) and tubastatin A (HDAC6 specific inhibitor), have been shown to promote oncolytic virus replication in tumors *in vivo* [35,36,42]. The current work is the first to demonstrate a clinically relevant, anti-cancer HDACi able to enhance oHSV therapy by elevating virus amplification *in vivo*. We speculate that direct action of Pano on tumor cells (*i.e.*, modulation of mRNA processing) underlay enhanced oHSV replication. However, Pano may have inhibited NK cell-mediated lysis of infected MM cells *in vivo* to prevent early virus clearance [48].

5. Conclusion

We present preclinical evidence that pan-HDACis can improve oHSV therapy of MM *via* augmenting virus entry and replication. This finding can be rapidly translated into the clinic given both HDACis and G47Δ are currently in clinical use. Future research should also test this combination approach in an immunocompetent setting since HDACis have been shown to modulate innate as well as adoptive immune responses [29].

Supplementary Material

Refer to Web version on PubMed Central for supplementary material.

Acknowledgements

We thank Shanawaz Mohhamed Ghouse for providing technical advice on animal studies, and Drs. Gregory R. Wojtkiewicz and Stephen P. Schmidt at the MGH mouse imaging core facility for performing bioluminescence imaging of mice.

Funding

This work was supported by the Meningioma Mommas (to Hiroaki W) and a grant from NIH (R01 NS032677 to RLM).

Data availability

The RNA sequencing data presented in this work is publicly available at NIH GEO as GSE210178.

References

[1]. Ostrom QT, Patil N, Cioffi G, Waite K, Kruchko C, Barnholtz-Sloan JS, CBTRUS statistical report: primary brain and other central nervous system tumors diagnosed in the United States in 2013–2017, Neuro Oncol. 22 (2020) iv1–iv96. [PubMed: 33123732]

[2]. Brastianos PK, Horowitz PM, Santagata S, Jones RT, McKenna A, Getz G, Ligon KL, Palescandolo E, Van Hummelen P, Ducar MD, Raza A, Sunkavalli A, et al. , Genomic sequencing of meningiomas identifies oncogenic SMO and AKT1 mutations, Nat. Genet 45 (2013) 285–289. [PubMed: 23334667]

[3]. Clark VE, Erson-Omay EZ, Serin A, Yin J, Cotney J, Ozduman K, Avsar T, Li J, Murray PB, Henegariu O, Yilmaz S, Gunel JM, et al. , Genomic analysis of non-NF2 meningiomas reveals mutations in TRAF7, KLF4, AKT1, and SMO, Science 339 (2013) 1077–1080. [PubMed: 23348505]

[4]. Chamberlain MC, Hydroxyurea for recurrent surgery and radiation refractory high-grade meningioma, J. Neurooncol 107 (2011) 315–321. [PubMed: 22127733]

[5]. Chamberlain MC, Tsao-Wei DD, Groshen S, Temozolomide for treatment-resistant recurrent meningioma, Neurology 62 (2004) 1210–1212. [PubMed: 15079029]

[6]. Johnson DR, Kimmel DW, Burch PA, Cascino TL, Giannini C, Wu W, Buckner JC, Phase II study of subcutaneous octreotide in adults with recurrent or progressive meningioma and meningeal hemangiopericytoma, Neuro Oncol. 13 (2011) 530–535. [PubMed: 21558077]

[7]. Nayak L, Iwamoto FM, Rudnick JD, Norden AD, Lee EQ, Drappatz J, Omuro A, Kaley TJ, Atypical and anaplastic meningiomas treated with bevacizumab, J. Neurooncol 109 (2012) 187–193. [PubMed: 22544653]

[8]. Norden AD, Ligon KL, Hammond SN, Muzikansky A, Reardon DA, Kaley TJ, Batchelor TT, Plotkin SR, Raizer JJ, Wong ET, Drappatz J, Lesser GJ, et al. , Phase II study of monthly pasireotide LAR (SOM230C) for recurrent or progressive meningioma, Neurology 84 (2015) 280–286. [PubMed: 25527270]

[9]. Norden AD, Raizer JJ, Abrey LE, Lamborn KR, Lassman AB, Chang SM, Yung WK, Gilbert MR, Fine HA, Mehta M, Deangelis LM, Cloughesy TF, et al. , Phase II trials of erlotinib or gefitinib in patients with recurrent meningioma, J. Neurooncol 96 (2010) 211–217. [PubMed: 19562255]

[10]. Raizer JJ, Grimm SA, Rademaker A, Chandler JP, Muro K, Helenowski I, Rice L, McCarthy K, Johnston SK, Mrugala MM, Chamberlain M, A phase II trial of PTK787/ZK 222584 in recurrent or progressive radiation and surgery refractory meningiomas, J. Neurooncol 117 (2014) 93–101. [PubMed: 24449400]

[11]. Reardon DA, Norden AD, Desjardins A, Vredenburgh JJ, Herndon JE 2nd, Coan A, Sampson JH, Gururangan S, Peters KB, McLendon RE, Norfleet JA, Lipp ES, et al. , Phase II study of Gleevec(R) plus hydroxyurea (HU) in adults with progressive or recurrent meningioma, J. Neurooncol 106 (2012) 409–415. [PubMed: 21938530]

[12]. Wen PY, Quant E, Drappatz J, Beroukhim R, Norden AD, Medical therapies for meningiomas, J. Neurooncol 99 (2010) 365–378. [PubMed: 20820875]

[13]. Wen PY, Yung WK, Lamborn KR, Norden AD, Cloughesy TF, Abrey LE, Fine HA, Chang SM, Robins HI, Fink K, Deangelis LM, Mehta M, et al. , Phase II study of imatinib mesylate for recurrent meningiomas (North American Brain Tumor Consortium study 01–08), Neuro Oncol. 11 (2009) 853–860. [PubMed: 19293394]

[14]. Champeaux C, Jecko V, Houston D, Thorne L, Dunn L, Fersht N, Khan AA, Resche-Rigon M, Malignant meningioma: an international multicentre retrospective study, Neurosurgery 85 (2019) E461–E469. [PubMed: 30566646]

[15]. Orton A, Frandsen J, Jensen R, Shrieve DC, Suneja G, Anaplastic meningioma: an analysis of the National Cancer Database from 2004 to 2012, J. Neurosurg 128 (2018) 1684–1689. [PubMed: 28731397]

[16]. Russell SJ, Peng KW, Bell JC, Oncolytic virotherapy, Nat. Biotechnol 30 (2012) 658–670. [PubMed: 22781695]

[17]. Esaki S, Nigim F, Moon E, Luk S, Kiyokawa J, Curry W Jr., Cahill DP, Chi AS, Iafrate AJ, Martuza RL, Rabkin SD, Wakimoto H, Blockade of transforming growth factor-beta signaling enhances oncolytic herpes simplex virus efficacy in patient-derived recurrent glioblastoma models, Int J. Cancer 141 (2017) 2348–2358. [PubMed: 28801914]

[18]. Jahan N, Lee JM, Shah K, Wakimoto H, Therapeutic targeting of chemoresistant and recurrent glioblastoma stem cells with a proapoptotic variant of oncolytic herpes simplex virus, Int J. Cancer 141 (2017) 1671–1681. [PubMed: 28567859]

[19]. Kanai R, Rabkin SD, Yip S, Sgubin D, Zaupa CM, Hirose Y, Louis DN, Wakimoto H, Martuza RL, Oncolytic virus-mediated manipulation of DNA damage responses: synergy with chemotherapy in killing glioblastoma stem cells, J. Natl. Cancer Inst 104 (2012) 42–55. [PubMed: 22173583]

[20]. Nigim F, Esaki S, Hood M, Lelic N, James MF, Ramesh V, Stemmer-Rachamimov A, Cahill DP, Brastianos PK, Rabkin SD, Martuza RL, Wakimoto H, A new patient-derived orthotopic malignant meningioma model treated with oncolytic herpes simplex virus, Neuro Oncol. 18 (2016) 1278–1287. [PubMed: 26951380]

[21]. Ning J, Wakimoto H, Peters C, Martuza RL, Rabkin SD, Rad51 degradation: role in oncolytic virus-poly(ADP-Ribose) polymerase inhibitor combination therapy in glioblastoma, J. Natl. Cancer Inst 109 (2017) 1–13.

[22]. Sgubin D, Wakimoto H, Kanai R, Rabkin SD, Martuza RL, Oncolytic herpes simplex virus counteracts the hypoxia-induced modulation of glioblastoma stem-like cells, Stem Cells Transl. Med 1 (2012) 322–332. [PubMed: 23197811]

[23]. Todo T, Ino Y, Ohtsu H, Shibahara J, Tanaka M, A phase I/II study of triple-mutated oncolytic herpes virus G47 in patients with progressive glioblastoma, Nat. Commun 13 (2022) 4119. [PubMed: 35864115]

[24]. Todo T, Ito H, Ino Y, Ohtsu H, Ota Y, Shibahara J, Tanaka M, Intratumoral oncolytic herpes virus G47 for residual or recurrent glioblastoma: a phase 2 trial, Nat. Med (2022).

[25]. Saha D, Wakimoto H, Peters CW, Antoszczyk SJ, Rabkin SD, Martuza RL, Combinatorial effects of VEGFR kinase inhibitor axitinib and oncolytic virotherapy in mouse and human glioblastoma stem-like cell models, Clin. Cancer Res 24 (2018) 3409–3422. [PubMed: 29599413]

[26]. Falkenberg KJ, Johnstone RW, Histone deacetylases and their inhibitors in cancer, neurological diseases and immune disorders, Nat. Rev. Drug Disco 13 (2014) 673–691.

[27]. Eckschlager T, Plch J, Stiborova M, Hrabeta J, Histone deacetylase inhibitors as anticancer drugs, Int. J. Mol. Sci 18 (2017).

[28]. Jenke R, Ressing N, Hansen FK, Aigner A, Buch T, Anticancer therapy with HDAC inhibitors: mechanism-based combination strategies and future perspectives, Cancers (Basel) (2021) 13.

[29]. Marchini A, Scott EM, Rommelaere J, Overcoming barriers in oncolytic virotherapy with HDAC inhibitors and immune checkpoint blockade, Viruses 8 (2016).

[30]. Nakashima H, Nguyen T, Chiocca EA, Combining HDAC inhibitors with oncolytic virotherapy for cancer therapy, Oncolytic Virother. 4 (2015) 183–191. [PubMed: 27512681]

[31]. Todo T, Martuza RL, Rabkin SD, Johnson PA, Oncolytic herpes simplex virus vector with enhanced MHC class I presentation and tumor cell killing, Proc. Natl. Acad. Sci. USA 98 (2001) 6396–6401. [PubMed: 11353831]

[32]. Cheema TA, Wakimoto H, Fecci PE, Ning J, Kuroda T, Jeyaretna DS, Martuza RL, Rabkin SD, Multifaceted oncolytic virus therapy for glioblastoma in an immunocompetent cancer stem cell model, Proc. Natl. Acad. Sci. USA 110 (2013) 12006–12011. [PubMed: 23754388]

[33]. Nigim F, Kiyokawa J, Gurtner A, Kawamura Y, Hua L, Kasper EM, Brastianos PK, Cahill DP, Rabkin SD, Martuza RL, Carbonell WS, Wakimoto H, A monoclonal antibody against beta1 integrin inhibits proliferation and increases survival in an orthotopic model of high-grade meningioma, Target Oncol. 14 (2019) 479–489. [PubMed: 31301014]

[34]. Lu Y, Stuart JH, Talbot-Cooper C, Agrawal-Singh S, Huntly B, Smid AI, Snowden JS, Dupont L, Smith GL, Histone deacetylase 4 promotes type I interferon signaling, restricts DNA viruses, and is degraded via vaccinia virus protein C6, Proc. Natl. Acad. Sci. USA 116 (2019) 11997–12006. [PubMed: 31127039]

[35]. Nguyen TL, Abdelbary H, Arguello M, Breitbach C, Leveille S, Diallo JS, Yasmeen A, Bismar TA, Kirn D, Falls T, Snoulten VE, Vanderhyden BC, et al. , Chemical targeting of the innate antiviral response by histone deacetylase inhibitors renders refractory cancers sensitive to viral oncolysis, Proc. Natl. Acad. Sci. USA 105 (2008) 14981–14986. [PubMed: 18815361]

[36]. Otsuki A, Patel A, Kasai K, Suzuki M, Kurozumi K, Chiocca EA, Saeki Y, Histone deacetylase inhibitors augment antitumor efficacy of herpes-based oncolytic viruses, Mol. Ther 16 (2008) 1546–1555.

[37]. Schoggins JW, Rice CM, Interferon-stimulated genes and their antiviral effector functions, Curr. Opin. Virol 1 (2011) 519–525. [PubMed: 22328912]

[38]. Katsura T, Iwai S, Ota Y, Shimizu H, Ikuta K, Yura Y, The effects of trichostatin A on the oncolytic ability of herpes simplex virus for oral squamous cell carcinoma cells, Cancer Gene Ther. 16 (2009) 237–245. [PubMed: 18949013]

[39]. Liu TC, Castelo-Branco P, Rabkin SD, Martuza RL, Trichostatin A and oncolytic HSV combination therapy shows enhanced antitumoral and antiangiogenic effects, Mol. Ther 16 (2008) 1041–1047. [PubMed: 18388912]

[40]. Cody JJ, Markert JM, Hurst DR, Histone deacetylase inhibitors improve the replication of oncolytic herpes simplex virus in breast cancer cells, PLoS One 9 (2014), e92919. [PubMed: 24651853]

[41]. Tatman PD, Wroblewski TH, Fringuello AR, Scherer SR, Foreman WB, Damek DM, Lillehei K, Youssef AS, Jensen RL, Graner MW, Ormond DR, High-throughput mechanistic screening of epigenetic compounds for the potential treatment of meningiomas, J. Clin. Med (2021) 10.

[42]. Nakashima H, Kaufmann JK, Wang PY, Nguyen T, Speranza MC, Kasai K, Okemoto K, Otsuki A, Nakano I, Fernandez S, Goins WF, Grandi P, et al. , Histone deacetylase 6 inhibition enhances oncolytic viral replication in glioma, J. Clin. Invest 125 (2015) 4269–4280. [PubMed: 26524593]

[43]. Berghauser Pont LM, Kleijn A, Kloezeman JJ, van den Bossche W, Kaufmann JK, de Vrij J, Leenstra S, Dirven CM, Lamfers ML, The HDAC Inhibitors scriptaid and LBH589 combined with the oncolytic virus delta24-RGD exert enhanced anti-tumor efficacy in patient-derived glioblastoma cells, PLoS One 10 (2015), e0127058. [PubMed: 25993039]

[44]. Hennig T, Djakovic L, Dolken L, Whisnant AW, A review of the multipronged attack of herpes simplex virus 1 on the host transcriptional machinery, Viruses 13 (2021).

[45]. Bryant HE, Wadd SE, Lamond AI, Silverstein SJ, Clements JB, Herpes simplex virus IE63 (ICP27) protein interacts with spliceosome-associated protein 145 and inhibits splicing prior to the first catalytic step, J. Virol 75 (2001) 4376–4385. [PubMed: 11287586]

[46]. Escudero-Paunetto L, Li L, Hernandez FP, Sandri-Goldin RM, SR proteins SRp20 and 9G8 contribute to efficient export of herpes simplex virus 1 mRNAs, Virology 401 (2010) 155–164. [PubMed: 20227104]

[47]. Sandri-Goldin RM, Hibbard MK, Hardwicke MA, The C-terminal repressor region of herpes simplex virus type 1 ICP27 is required for the redistribution of small nuclear ribonucleoprotein particles and splicing factor SC35; however, these alterations are not sufficient to inhibit host cell splicing, J. Virol 69 (1995) 6063–6076. [PubMed: 7666511]

[48]. Alvarez-Breckenridge CA, Yu J, Price R, Wei M, Wang Y, Nowicki MO, Ha YP, Bergin S, Hwang C, Fernandez SA, Kaur B, Caligiuri MA, et al. , The histone deacetylase inhibitor valproic acid lessens NK cell action against oncolytic virus-infected glioblastoma cells by inhibition of STAT5/T-BET signaling and generation of gamma interferon, J. Virol 86 (2012) 4566–4577. [PubMed: 22318143]

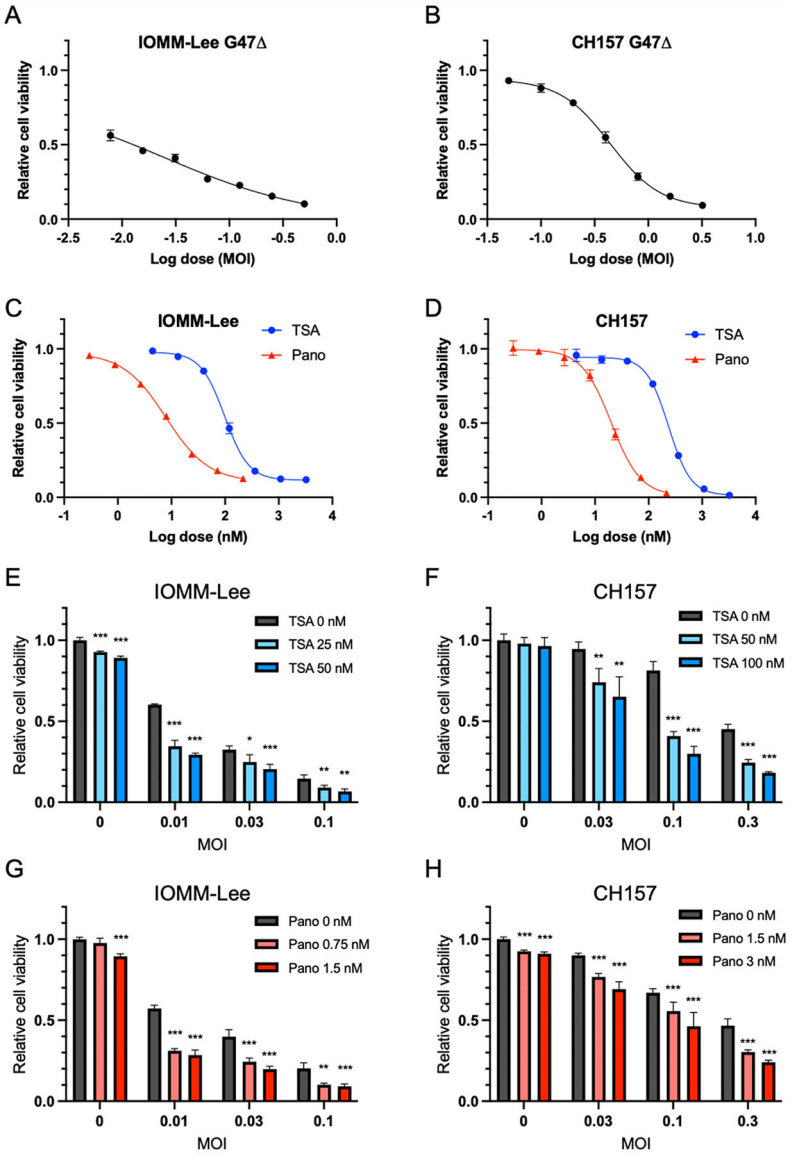

Fig. 1.

Low dose HDAC inhibitors enhance G47Δ-mediated killing of malignant meningioma cells *in vitro*. **A and B,** MTS cell viability assay showing dose-dependent responses to oHSV G47Δ in IOMM-Lee (A) and CH157 (B) cells. Assay was done 3 days post-infection. **C and D,** MTS cell viability assay showing dose-dependent responses to HDAC inhibitors Trichostatin A (TSA) and Panobinostat (Pano) in IOMM-Lee (C) and CH157 (D) cells. Assay was done 3 days after exposure to each drug. **E-H,** MTS cell viability assay showing the ability of a minimally toxic dose of HDAC inhibitors to sensitize malignant meningioma cells (IOMM-Lee, E and G; CH157, F and H) to G47Δ-mediated killing. Cells were pre-exposed to the indicated HDAC inhibitor for 5 h when cells were infected with G47Δ. MTS assay was done 3 days later. Mean and standard deviation (bars) of cell viability relative to untreated control cells are presented. *, $p< 0.05$; **, $p< 0.01$; and ***, $p< 0.001$ compared with no HDAC inhibitor in each group (Student t-test).

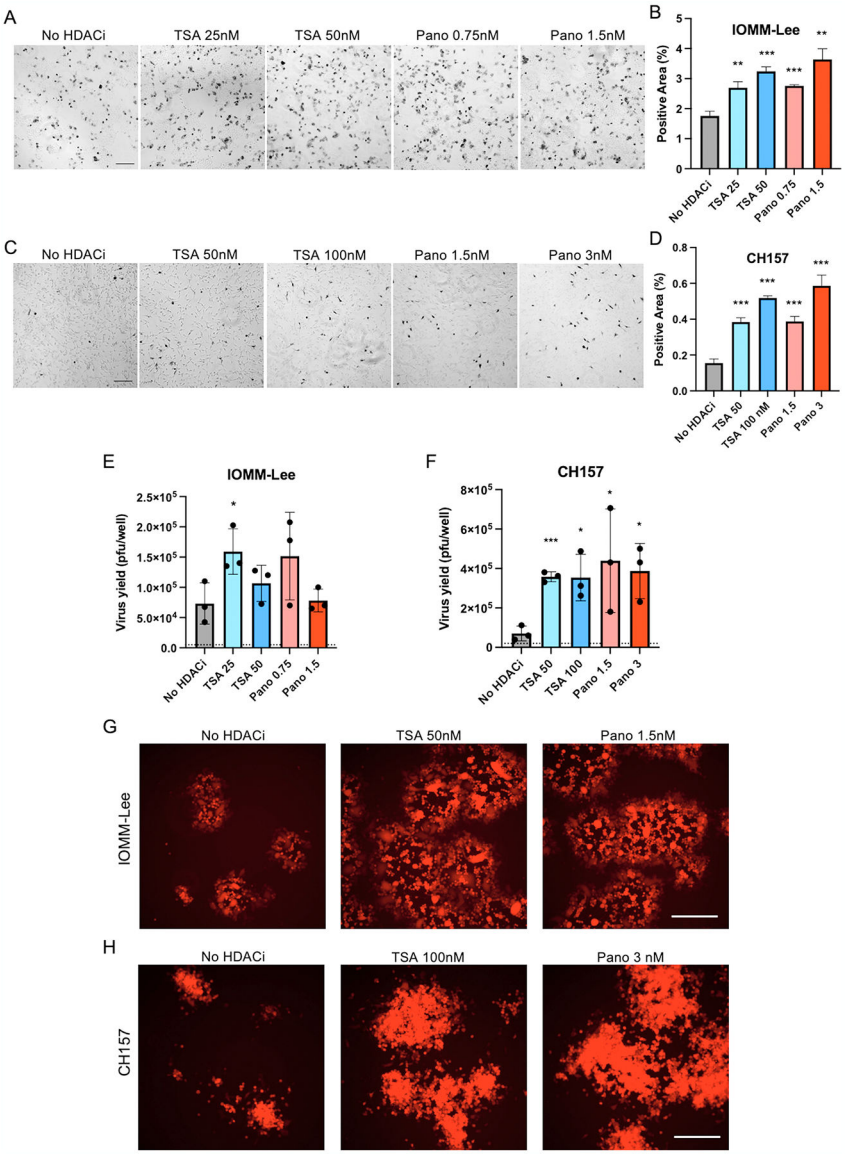

Fig. 2.

Pan-HDAC inhibitors enhance entry, replication, and spread of G47Δ in malignant meningioma cells *in vitro*. **A-D,** Virus infectability assay. A and B, IOMM-Lee cells. C and D, CH157 cells. A and C, Representative microscopic pictures showing x-gal positive cells in dark (black). Scale bars: 100 μm. B and D, Quantification of triplicate images. **E and F,** Virus yield assay. IOMM-Lee cells (E) and CH157 cells (F) were exposed to HDAC inhibitors at indicated concentration (nM), followed 5 h later by infection with G47Δ at MOI= 0.05 (IOMM-Lee) or 0.2 (CH157). Cells and culture media were collected at 24 h (IOMM-Lee) or 40 h (CH157) post-infection for determining virus yield. Dotted line: virus input. **G and H,** Virus spread assay. IOMM-Lee (G) or CH157 cells (H) were infected with G47Δ-mCherry at MOI= 0.1. Microscopic images for mCherry fluorescence were captured at 28 h (IOMM-Lee) and 45 h (CH157) post infection. Scale bars: 100 μm. *, $p< 0.05$; **, $p< 0.01$; ***, $p< 0.001$ compared with no HDAC inhibitor in each group (Student t-test).

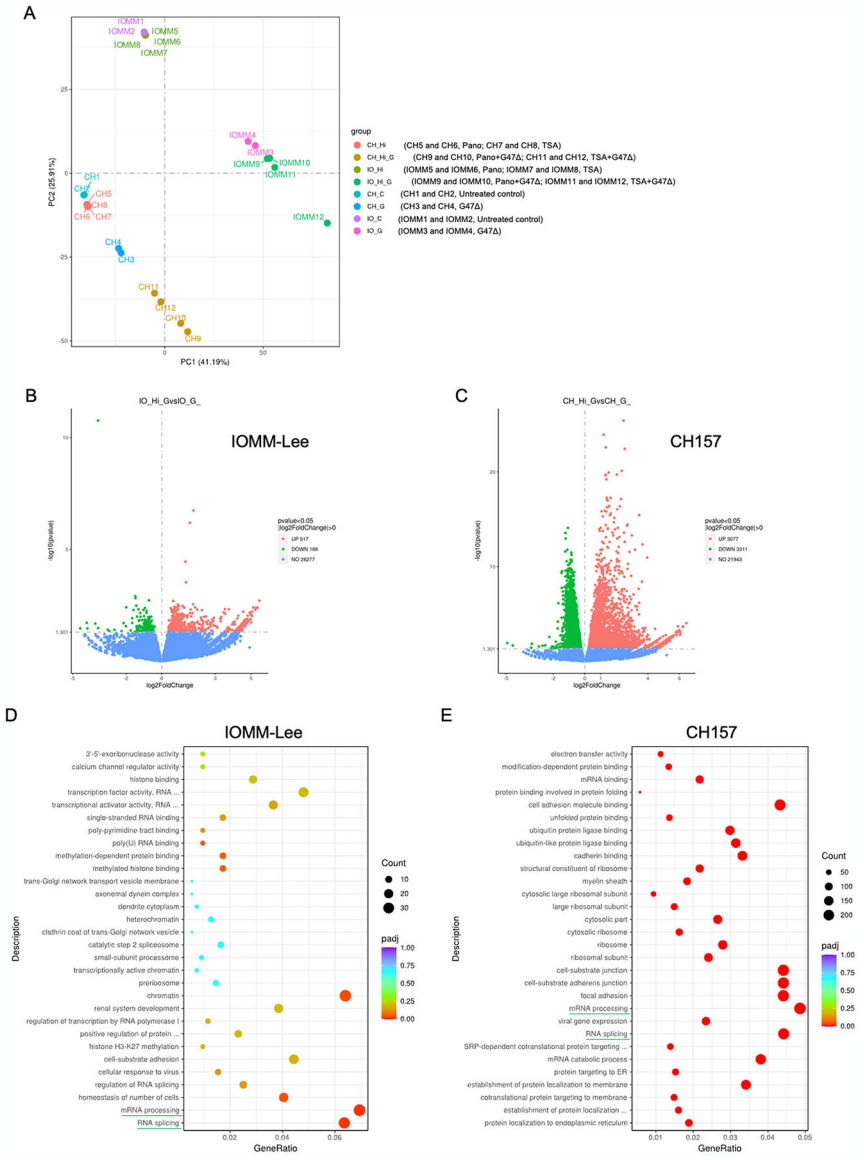

Fig. 3.

RNA sequencing analysis of the impacts of HDAC inhibitors on G47Δ-induced transcriptomics. **A**, Principal component analysis. IOMM-Lee cells (IO, IOMM), CH157 cells (CH). Numbers that follow cell type denote: mock-treated control (C), 1 and 2; G47Δ alone, 3 and 4; Panobinostat (Pano), 5 and 6; Trichostatin A (TSA), 7 and 8; Pano+G47Δ, 9 and 10; and TSA+G47Δ, 11 and 12. G47Δ, G; HDAC inhibitors (Pano and TSA), Hi. Symbol coloring on right is based on grouping in which Pano and TSA groups were combined as Hi. **B and C,** Volcano plots, comparing HDAC inhibitors+G47Δ (Hi_G) *vs.* G47Δ alone (G) in IOMM-Lee cells (B) and CH157 cells (C). **D and E,** Gene Ontology (GO) enrichment analysis, comparing HDAC inhibitors+G47Δ *vs.* G47Δ alone in. D, IOMM-Lee cells (D) and CH157 cells (E). The most significant 30 GO terms are displayed. padj, p adjusted.

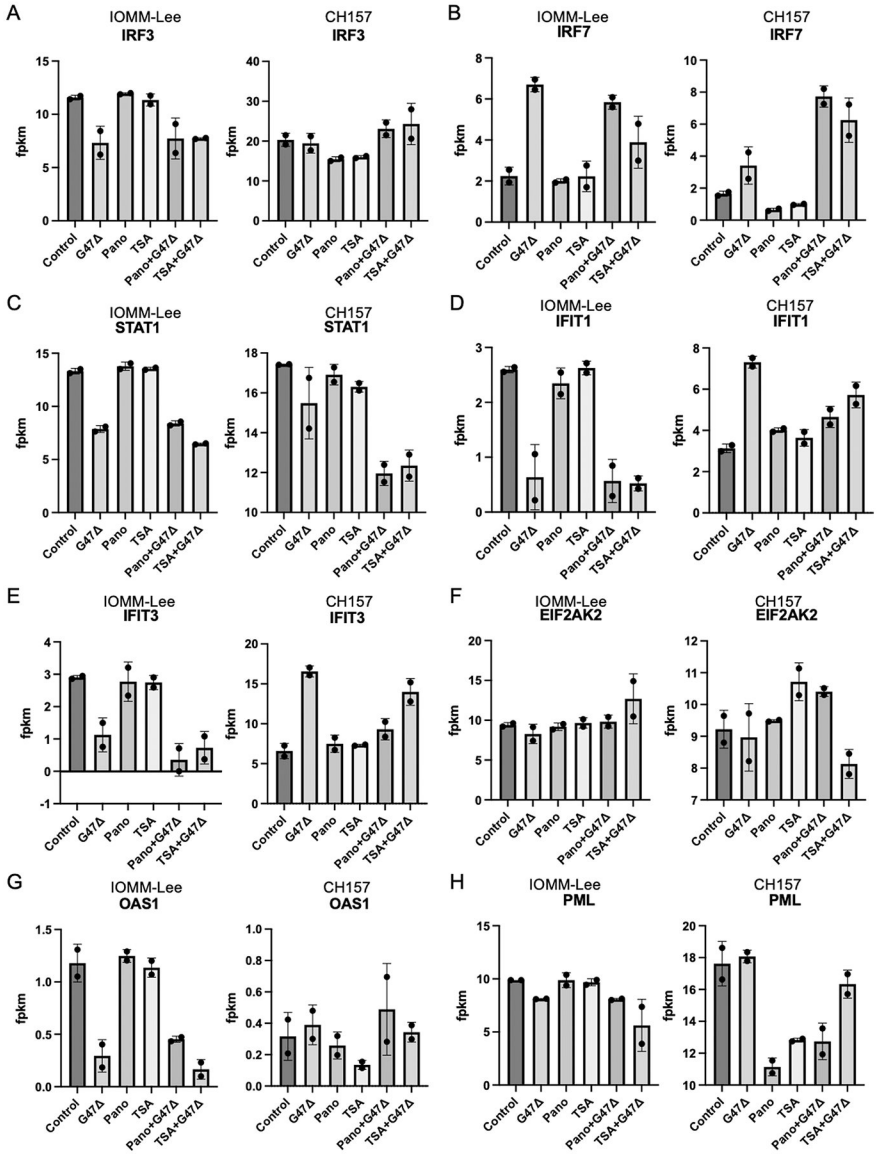

Fig. 4.

Impact of HDACis on the expression of genes involved in interferon-mediated innate anti-viral responses. Analysis of the RNA sequencing data presented in Fig. 3. **A,** IRF3, **B,** IRF7, **C,** STAT1, **D,** IFIT1, **E,** IFIT3, **F,** EIF2AK2 (PKR), **G,** OAS1 and **H,** PML.

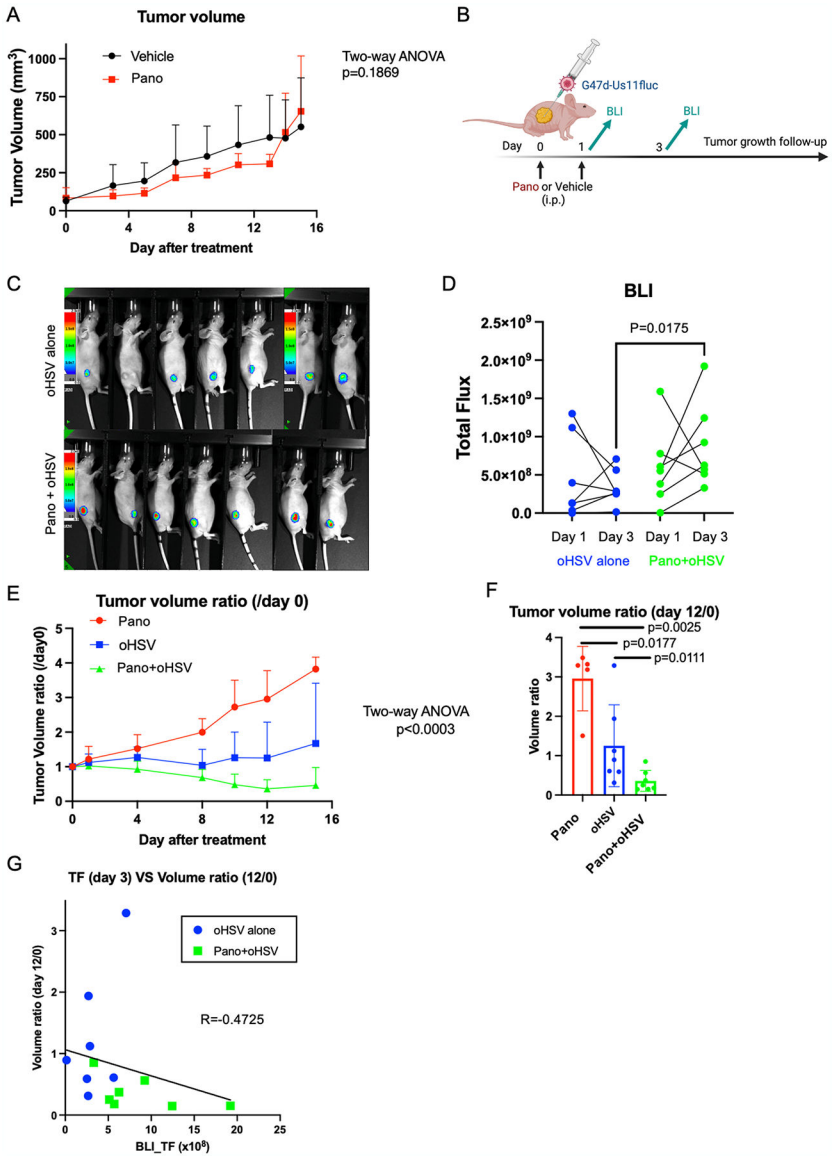

Fig. 5.

Pan HDAC inhibitor enhances replication and therapeutic effects of oHSV in malignant meningioma. **A**, Tumor growth curves of IOMM-Lee flank xenografts treated with vehicle or Panobinostat (Pano). **B,** Schema showing the experimental design; Pano, 30 mg/kg on Days 0 and 1, and G47ΔUs11fluc injected intra-tumorally at 3×10^5 pfu on Day 0, 5 h after the first Pano dosing. BLI, Bioluminescence. Created by BioRender.com. **C,** BLI on Day 3. The group that received Pano alone was not subjected to BLI. **D,** Changes in total flux signal from Day 1 to Day 3. **E,** Tumor growth curves of the 3 groups: Pano, G47ΔUs11fluc (oHSV) and Pano+G47ΔUs11fluc. Tumor volume relative to Day 0 is presented to assist comparison between groups. **F,** Tumor volume ratio (Day 12/Day 0), comparing the 3 groups. Each dot represents a tumor. **G,** Spearman correlation coefficients to show relationship between Day 3 BLI total flux (TF)(x-axis) and tumor volume ratio (Day

12/Day 0)(y-axis) from the G47ΔUs11fluc (oHSV) and Pano+oHSV groups together. Each dot represents a tumor.